VIRGO COLLABORATION, KAGRA COLLABORATION
==========
LIGO SCIENTIFIC COLLABORATION

VIR-0507A-13	LIGO-T1300841–v1	JGW-T1301693-v0

Report from the June 2013 Scattering Workshop at GEO

Kate Dooley, Tomo Akutsu, Yoichi Aso, Romain Bonnand, Sheila Dwyer, Irene Fiori, Hartmut Grote, Jan Harms, Jon Leong, Harald Lück, Julien Marque, Denis Martynov, Mirko Prijatelj, Robert Schofield, Emil Schreiber, Jake Slutsky, Bas Swinkels, Matteo Tacca, Gabriele Vajente, Michal Was, Holger Wittel

Distribution of this document:

LIGO Scientific Collaboration
Virgo Collaboration
Kagra Collaboration

http://www.ligo.org/
http://www.virgo.infn.it/
http://gwcenter.icrr.u-tokyo.ac.jp/

Contents

1 Introduction

GEO hosted the 3rd of a series of international commissioning workshops aimed at bringing together commissioners from each of the ground-based detectors (LIGO, Virgo, Kagra, and GEO) to discuss and actively work on specific problems common to all interferometers. The selected focus topic for this workshop was scattered light, one of the problems that was encountered during the commissioning of all large scale gravitational-wave detectors. Since 2nd generation GW detectors aim for significantly increased sensitivities at low frequencies, stray light will be even more problematic. From the first workshop report [1]:

"The diagnosis and mitigation of noise from backscattered light are complicated techniques which are not well documented and require several years of interferometer experience to internalize. In order to share these techniques we will have a commissioning session at GEO aimed at scattered light reduction with a participant from each of the interferometers. It will be advantageous to share, in a thorough way, all of our techniques for estimating and mitigating scattered light noise."

In order to best share our techniques, we decided to spend some days doing actual noise-hunting work at GEO. Local commissioners were available to take part and provide support to the visitors.

This report is a summary of the discussions and work carried out during the workshop. The first and last days were held at the Institute and the middle three days at GEO itself. Participants gave presentations on the first day so that we could share experiences and establish a common language. The detailed agenda is found in Appendix A. The wiki page for the workshop also contains the presentations [2]. Details of each of the experiments can be found in the GEO-HF logbook.

2 The scattering process

Scattered light becomes a problem in GW detectors when light that leaves the main beam path is phase modulated and then rejoined with the main beam. This phase modulation of the carrier TEM00 mode is exactly what a GW also does, thus making scattered light a technical noise source. GW detectors are very sensitive to scattered light: even just one scattered photon every 100 seconds is enough to destroy our sensitivity.

A sinusoidal phase modulation of frequency Ω and amplitude m of an electric field with frequency ω_0 and amplitude E_0 can be described as:

$$E = E_0 \exp\left(i(\omega t + m\cos\left(\Omega t\right))\right). \tag{1}$$

Using the identity

$$\exp\left(iz\cos\left(\phi\right)\right) = \sum_{k=-\infty}^{\infty} i^k J_K(m) \exp\left(ik\phi\right), \tag{2}$$

where $J_k(m)$ are Bessel functions of the first kind, we can then write the phase modulated

field as

$$E = E_0 \exp(i\omega_0 t) = \sum_{k=-\infty}^{\infty} i^k J_K(m) \exp(ik\Omega t). \quad (3)$$

There are two different regimes in which we typically think about scattering: high frequency, low amplitude motion of the scattered light, and low frequency, large amplitude motion. The former produces a line in the spectrum and the latter produces what we typically call a 'scattering shelf' (or 'Nudeln' at GEO). The frequency of the 'knee' of the scattering shelf is determined by the maximum velocity of the phase modulator and the wavelength of the light:

$$f_{\max} = v_{\max}/(\lambda/2). \quad (4)$$

3 Experiments carried out at GEO

We spent three days at the site, carrying out experiments to hunt for scattered light, and making noise projections when possible. The work was guided in part by findings the local team had already made in the previous months, such as particularly high sensitivity at the output chamber and the identification of a group of peaks around 230 Hz that vary in amplitude as well as in frequency. These were the focus of some chamber shaking experiments, and other experiments evaluated the general picture of scattered light coupling or specific subsystems.

3.1 Beam tube excitation at 300 and 555 m

We laid the shaker (a modified loudspeaker) on top of the East tube vacuum pipe at 300 m and at 555 m, and one accelerometer rigidly attached to the pipe about 1 m away and directed along the beam. A saw-tooth, 6.3 Hz-rate signal was sent to the shaker. We recorded the accelerometer signal for one (three, for the 555 m setup) 32 s-long periods with the shaker (injection on) and as many quiet ones (injection off). We noticed that our talking/clapping-hands could excite significant pipe vibrations. Shaker injections excited the pipe at comb frequencies from 19Hz to 1024 Hz with 6.3 Hz spacing, about a factor 100 above its quiet natural vibration. We then searched the h sensitivity signal for noise correlated with our injections but found none. The possible small noise excess noticed in a few frequency bins actually seemed consistent with random noise: indeed it is neither coincident with none of the comb's frequencies nor is it reproduced in all of our injections.

We used the data to produce an upper limit transfer function and an upper limit noise projection. The upper limit TF is computed taking the ratio of the ASD of the sensitivity over the ASD of the accelerometer as recorded during the injection. Only the comb bin frequencies are used for the computation, and a 10 s time window is used for the ASD. The upper limit projection is this TF multiplied by the ASD of the accelerometer quiet record.

The projection is shown in Fig. 1 gives an indication of maximum contribution of the noise due to light scattered by the tube walls/baffles back into the interferometer, and it says it is likely at least a factor 100 below the current sensitivity. This limit could of course be improved by increasing the shaking amplitude (yet we were quite close to shaker saturation)

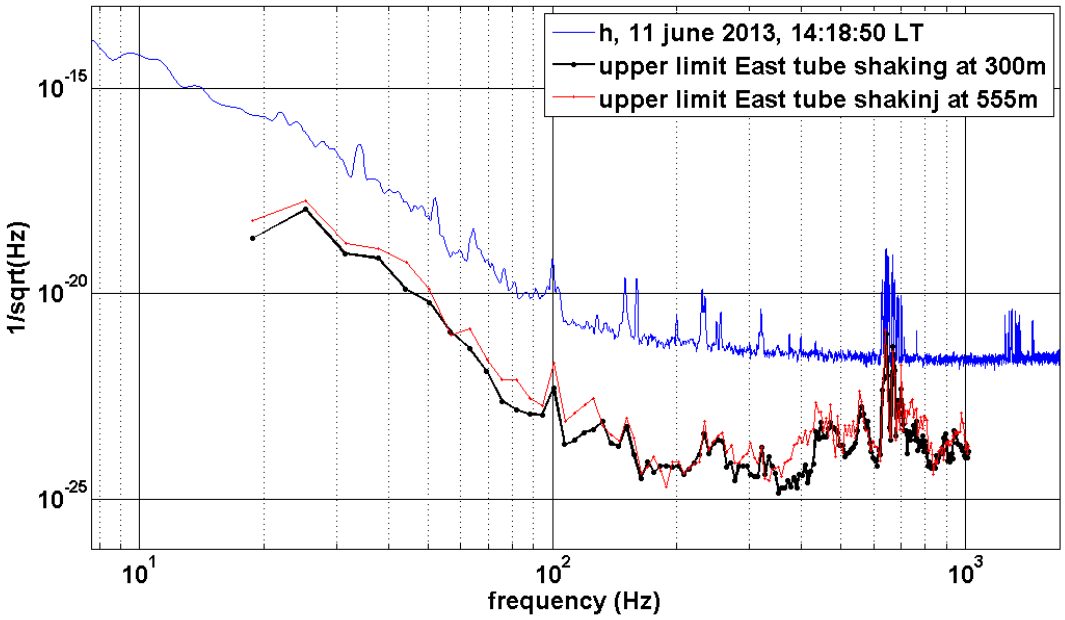

Figure 1: Beam tube shaking projection.

or (better) doing longer injections and then use a higher frequency resolution. However, it seems to us that the following considerations apply to the present result. Baffles along the pipe are the most likely locations for light back-scattering. In our experiment we could not tell how close the shaker was to the nearest baffle nor how much we excited all individual baffles along the pipe. Possibly the nearest baffle vibration was a bit less than what we measured, so the upper limit noise projection might indeed be a bit too optimistic for that specific baffles. In addition, there might be more critical baffles that we have not projected. It might be helpful to get an idea of the decay length of vibrations along the pipe. Presumably, due to the strong damping of the rock-wool around the tube, we were shaking only a short section (on the order of a meter up to a few at most), hence an upper limit projection of the whole tube would be a factor of a few hundred higher.

3.2 Acoustic noise injections

We injected acoustic noise in the central hall, taking care not to saturate the microphone. We used a loudspeaker, which was placed high in the corner of the central station. We injected single lines, swept-sines, a square wave, a sawtooth signal, and broadband noise in the 100-300 Hz band. The injections could increase significantly the ambient noise and were very well visible in the GEO sensitivity. Nevertheless, during broadband excitations quite low coherence was observed between the microphone and h signals. This indicates that there is a strong non-linear or non-stationary coupling, which agrees very well with the observed sideband production when we injected single lines.

We computed two noise projections: one using the sawtooth injection transfer function and

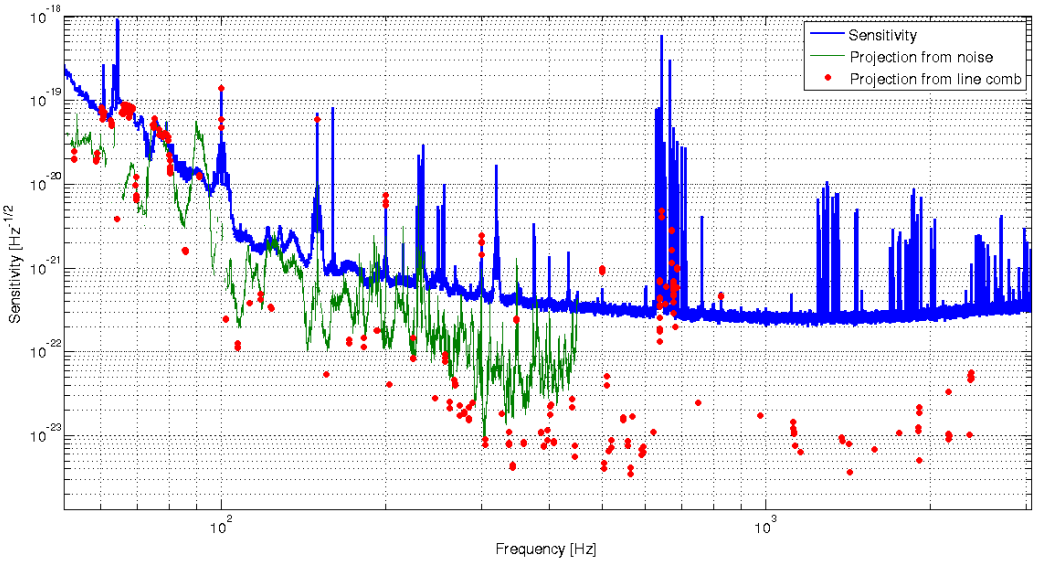

Figure 2: Acoustic noise projection.

one using the broadband noise transfer function. We made the transfer functions by taking the ratio of the sensitivity spectrum over the microphone spectrum while injecting noise, and set a threshold. Only points where the sensitivity is worse by at least 20% with respect to quiet condition were considered for the broadband injection; and for the sawtooth projection we considered only the points where the coherence was higher than 50%. This corresponds to the frequency of linear coupling for each peak.

The results are shown in Fig. 2. The projection from broadband noise is almost everywhere larger than the one with lines: this again indicates that the coupling is mainly non-linear or non-stationary. To better understand the non-stationarity, we computed a spectrogram of the sensitivity while injecting the noise. The result showed a lot of relatively fast non stationarity, even though it is difficult to identify any periodic behavior.

The effect of non-stationarity, however, is very well visible with a single line injection, especially at low frequency. In Figure 3 we compare the sensitivity while injecting a 120 Hz line (blue curve) with some artificial signals built by taking the product of a pure 120 Hz sinusoid with the signal recycling mirror (MSR) angular signals. These synthetic signals reconstruct quite well the sidebands visible in the sensitivity. We can conlude that a good portion of the non-stationary is due to alignment fluctuations. This could have been expected since the beginning.

3.3 Tapping / local excitation in TCOc (output chamber)

While listening to $h(t)$ using the wireless headphones, we did some tapping tests around various tanks in the center building and found that, in particular, the flange between TCOc and TCOb was very sensitive. An audio file demonstrating what we could here can be found on the workshop wiki [2]. We thus followed up this finding with a more detailed investigation by shaking the TCOc (OMC+PD) chamber to make a seismic noise projection of scattering

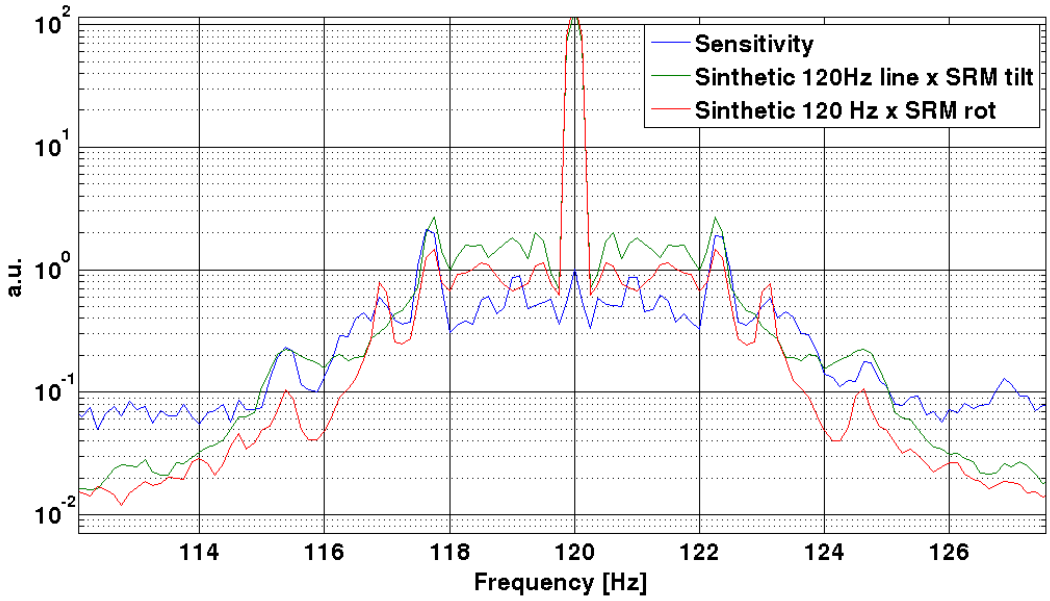

Figure 3: Demonstration that the sidebands observed around single line injections are due to residual MSR angular motion modulating the lines.

to $h(t)$.

The setup is shown both schematically and with a photo in Figure 4. A shaker and a 3-axis accelerometer are fixed to the chamber, where the shaker is used to mimic ground vibrations and the accelerometer as a witness of the actual motion of the chamber. Figure 5 shows the results of a linear projection of accelerometer data from a quiet time to $h(t)$ using a transfer function obtained from a saw-tooth injection.

Based on past work at GEO, we know the angle of incidence of the output beam on the viewport between TCOb and TCOc to plays a large role in the level of backscatter. We tried to measure the resonance of the viewport type that is between TCOb and TCOc. We tried tapping the flange and looking for resonances and only found strong ones in the kHz range. The most prominent one that seems to be related to a bending mode of the window is at 1.96 kHz. We also tried acoustic injections and shaking tests, but these were not very conclusive. In any case there was no low frequency resonance to be found anywhere.

3.4 Other chamber shaking experiments

We used the small shaker to shake several of the vacuum chambers in the corner station in order to search for sources of features in h(t) that might be associated with scattering. If the chambers are not rigidly connected to the floor or to other chambers at the shaking frequencies, then a shaker on a chamber will increase the motion of that chamber more than it increases the motion of the floor or other chambers. The chamber in which the $h(t)$ feature is produced is likely the chamber with the greatest increase in $h(t)$ peak height relative to increase in chamber motion. Practical considerations such as shaking on only one axis mean

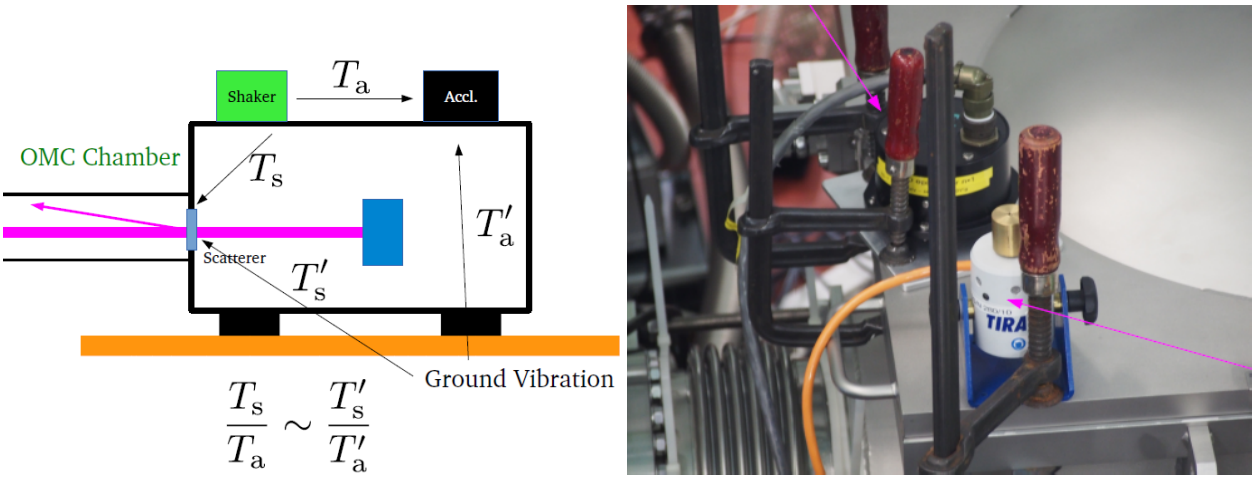

Figure 4: Left: Diagram showing the principle behind measuring a transfer function for projecting ground motion to strain. Right: Photograph of the actual setup. The upper arrow points to the accelerometer and the lower arrow to the shaker.

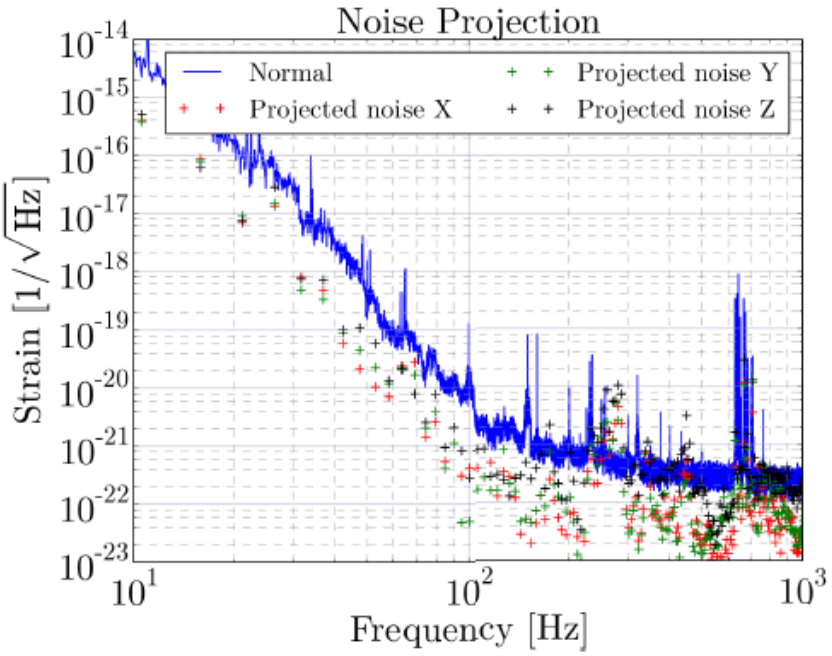

Figure 5: Output chamber (TCOc) shaking projection.

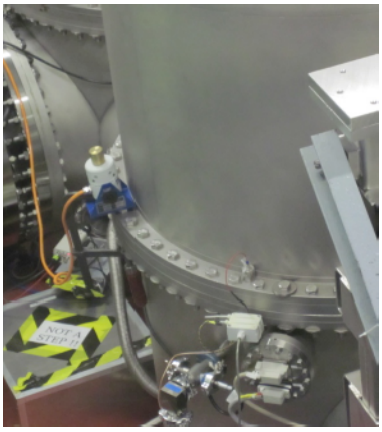

Figure 6: Photo showing an example of how the shaker and accelerometer were mounted to the chambers. The chamber pictuered here is TCN, which houses the north arm end mirror.

that the test is not infallible, and it may occasionally produce false alarms. Figure 6 shows a picture of the shaker on a chamber.

Figure 7 shows sample $h(t)$ and accelerometer spectra for shaking experiments at several of the chambers, with a focus around the cluster of 230 Hz lines. Because the amplitude of the 230 Hz group of peaks in h(t) varies so much, our procedure was to alternate between shaking and not-shaking several times at each site. All of the shaking spectra are plotted in red and all of the nominal spectra are plotted in blue. If all of the red traces are higher than all of the blue traces, there is a good indication that shaking increased the amplitude of the peak.

Two of the large spectral lines in the 230 Hz region, at about 228.5 and 229.8 Hz, appear to be associated with components in the TCN chamber, the chamber that holds the North arm test mass. Figure 7 shows that the increase in peak amplitude per increase in chamber motion is larger for shaking of TCN than for shaking of the nearest neighboring chamber and also shows that no increase is evident when two next nearest neighbor chambers are shaken. The small increase in amplitude associated with shaking TCC caused us to hypothesize that the peaks might be associated with this chamber before we found that the peaks were even more excited when we shook the TCN chamber.

Note that there is a peak at 245.8 Hz with broad side bands in Figure 7 that is most excited when TCC is shaken. The broad side bands of this peak are typical of peaks produced by backscattering into the interferometer arms where other motions modulate the phase variation from motion of the backscattering object. The broad sidebands of the 245.8 Hz peak contrast with the nearly sideband-free peaks just below 230 Hz. These sideband-free peaks at 228.5 and 229.8 are more likely to be produced by jitter coupling, clipping coupling or other coupling that does not tend to produce large side bands. The results were reproducible, even when the shaker and accelerometer were mounted at different positions on the chambers. The repeated measurements were made during different locks and separated in time by measurements at other chambers.

In addition to two of the 230 Hz lines, chamber shaking also suggested the chambers that contained the sources of some of the other smaller lines in h(t) and these are listed, along

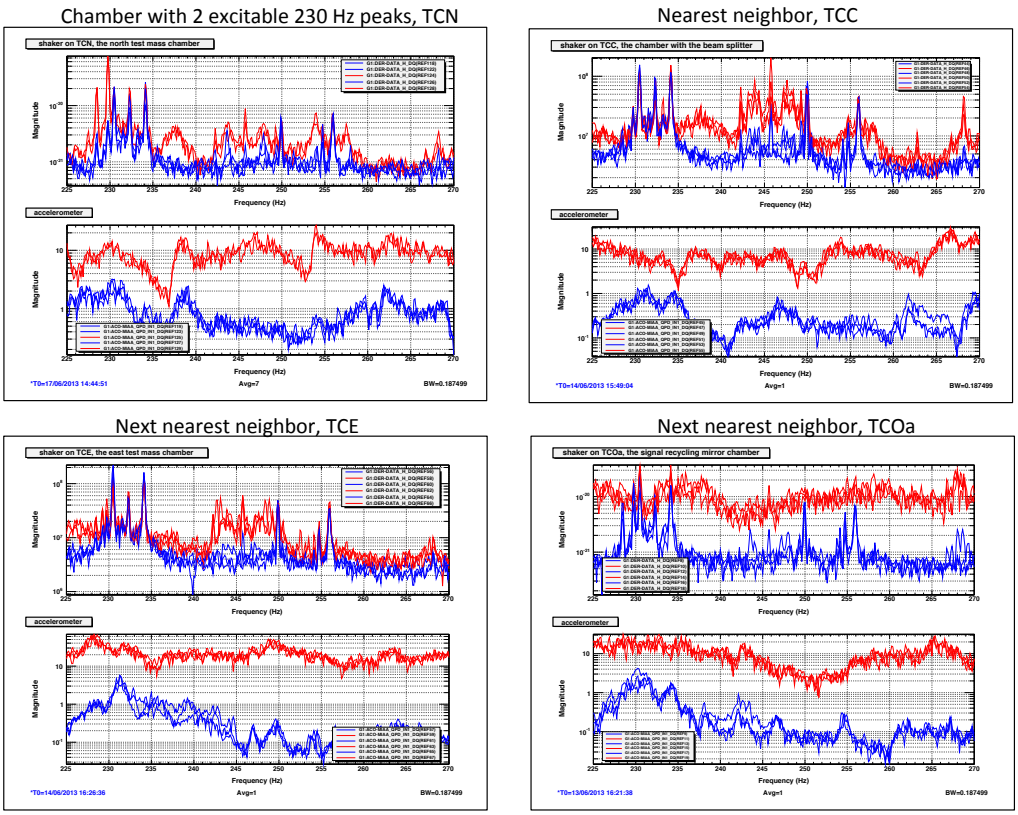

Figure 7: Sample chamber shaking measurements. All of the shaking spectra are plotted in red and all of the nominal spectra are plotted in blue. The upper panels of each plot show h and the lower panels are the accelerometer signals.

Table 1: List of dominant lines in h(t) identified by chamber shaking. The candidate chamber is the chamber with the greatest increase in peak amplitude per increase in chamber motion. The peak height/background level is at 0.19 Hz resolution, without shaking, and <= 1 indicates peak was not seen in h(t) without shaking. The final column indicates whether there are large side bands indicative of backscattering into the arms.

peak freq.	peak height / background level	candidate chamber	backscatter?
228.5	5 to 40 (varies)	TCN	no
229.8	5 to 40 (varies)	TCN	no
79	1.4	TCOa	yes
206	1.3	TCIb	yes
215.1	1.3	TCIb	yes
192.8	1.3	TCN	yes
245.8	<= 1	TCC	yes

with the 230 Hz lines, in Table 1, ordered by size in h(t) during normal operation.

Because of limited time, we only tested the small shaker for direct magnetic coupling at one of the chambers (by lifting it off of the chamber to reduce shaking coupling but keeping it near so magnetic coupling would be about the same), finding no evidence of magnetic coupling. Ideally we would do this at each chamber, or, avoid the possibility of magnetic coupling by using a piezo shaker instead of a voice coil. Because we were unable to do this, the possibility of magnetic coupling should be kept in mind - though it is unlikely because the increases in peak amplitude that we found were consistent with the increases in motion of the chambers as measured by the accelerometer. Of course even in the unlikely event that magnetic coupling dominated, this technique would still point to the chamber that contains the source of the peak because the field will be strongest in the chamber with the attached shaker/magnetic field generator.

3.5 Squeezing backscatter (by sqz. frequency shift in audio band)

We did an investigation of scattered power from the squeezer by injecting squeezing with the squeezer laser offset in frequency. If there is stray light generated on the squeezer table that enters the interferometer, it appears as a peak in the spectrum at the offset frequency. Light that scatters out of the interferometer, into the OPO, and back to the interferometer will undergo difference frequency generation in the OPO, and create a peak at twice the offset frequency [3, Sec. 6.3.3].

We repeated the experiment for a few different levels of injected squeezing, as well as at for a few different offset frequencies, where we chose frequencies at clean places within the h spectrum. We always saw a small peak at the offset frequency, and a larger one at twice the offset frequency. This indicates that there is a small amount of stray light originating on the squeezer itself, and more of the scattered light is scattered towards the squeezer from the interferometer. Figure 8 shows example spectra of h during the experiment.

To attempt to narrow down the source of on-board scattering, we unlocked the green mode cleaner, and saw that the $2f$ peak disappeared as expected, while the $1f$ peak remained,

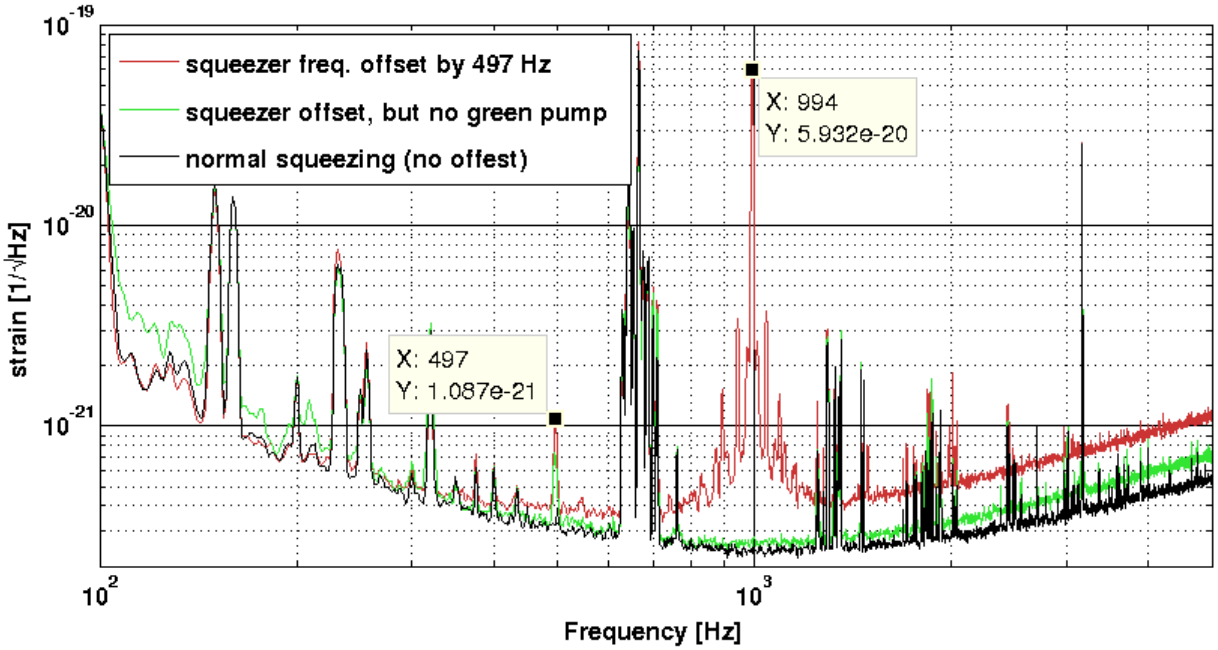

Figure 8: Example spectra of h during squeezer backscatter experiment. Shot-noise-limited sensitivity is worse with the frequency offset because the squeezing angle is rotating quickly and thus producing broadband anti-squeezing. The amplitudes of the f and $2f$ lines can tell us the power in the scattered light.

meaning that the scattered light originating from the squeezer is not coupled through the green path.

The shape of the spectrum around the lines together with the line amplitude can be used to make a noise projection.

3.6 Inducing scattering shelves

3.6.1 Longitudinal excitation of the output beam

This is an experiment to study the longitudinal excitation of BDO2 over many fringes, at low (below pendulum resonances) frequency. We put a large amplitude injection on BDO2 longitudinal near the resonance. This is to check the level of the scattering back from TCOc to see if it changed.

The data was analyzed using the standard formula for scattered light $h_{scat} = G_1 \sin(4\pi z_{scat}/\lambda)$, which is valid for light hitting a mirror under normal incidence. For the motion of the mirror, we take $z_{scat} = KV_{inj}$. Fitting the shoulder-frequency of the loudest injection, we get $K = 2.65 \times 10^{-08}$ m/V. Fitting the height of the shelf yields $G_1 = 2.5 \times 10^{-19}$. The fitting is not very accurate, some low-frequency noise should be added to make a smooth shelf and get a better projection. Using the same parameters, the shelf of the intermediate injection is predicted reasonably well. The weakest injection is not seen in the sensitivity.

For the loudest injection, a small bump could also be seen at higher frequencies, this might

be the 'double-bounce scattered light' or second harmonic arches. Fitting this bump with $h_{scat} = G_2 \sin(8\pi z_{scat}/\lambda)$ gives $G_2 = 9 \times 10^{-21}$.

Reading the corner frequency and amplitude of the shoulder from the figure of last year's figure gives $G_1 = 3.75 \times 10^{-18}$, so the recent work lowered the coupling factor by a factor 15. The gain K was probably different since different cabling was used.

Still to do is a noise-projection in quiet conditions, but this requires an accurate motion spectrum of all the optics between the interferometer and the OMC.

3.6.2 Longitudinal excitation of the input beam

We put longitudinal excitations to BDIPR (the suspended steering mirror between the input MCs (and suspended modulation bench) and the power recycling mirror). It was known beforehand that a weak parasitic optical cavity exists between the suspended modulation bench and the (further downstream located) power recycling mirror: Weak fringes can be observed in reflection of the power recycling mirror, which are expected to slightly contaminate the laser frequency control signal.

The aim of this injection was to possibly make scattering shelves in h, and to compare the fringe speed needed for a significant coupling to h with typical ambient fringe speeds. Sine wave injections, mainly around 300 mHz were used. A residual coupling into rotational (yaw) motion of the mirror was reduced by (better) diagonalizing the input matrix, which allowed the use of larger excitation amplitudes. A typical amplitude we used corresponeded to about 70 fringes peak-to-peak. The corresponding maximum fringe speed was $60*2*300\text{mHz}*\pi/2 = 66\text{Hz}$.

We clearly saw arches at this frequncy, and double bounce arches at twice the frequency, with the maximum frequency of the arch at times where the speed of the actuation is the largest. A comparison with the fringe speed of about 2-3 fringes per second under normal ambient conditions lets us conclude that the resulting coupling to h is far from limiting.

4 Summary

We brought together commissioners from each of Kagra, Virgo, LIGO, and GEO who have had experiences with identifying, finding and mitigating scattered light. We shared with one another stories of our particular scattered light problems and worked on identifying a common language to talk about scattered light. We identified the techniques typically used for globally characterizing the scattered light situation, and for mitigating the problem. We carried out familiar experiments, but with new collaborators and/or with a new detector, thus strengthening some of the principles we already knew as well as giving us some new ideas. Working one on one with commissioners from other detectors helps us understand each other better and forms an atmosphere conducive to opening up discussion in the future for the common challenges we will all face. We found the style of introductory talks on the first day, followed by several days of work interspersed with group discussions to be effective for a workshop.

References

[1] R. Adhikari et al. Report on GW Commissioning Meeting (2012 Cascina). Technical Report T1200464, LIGO Laboratory, October 2012.

[2] Workshop wiki page. https://nodus.ligo.caltech.edu:30889/wiki/doku.php?id=june2013.

[3] Sheila Dwyer. *Quantum noise reduction using squeezed states in LIGO*. PhD thesis, M.I.T., 2013.

A Agenda

Monday (at AEI, Seminar room 103, 3401):

- 9:30 structure of the workshop (Kate, Jon, Hartmut)
- 9:45 Introduction to scattering (Harald)
- 10:30 'Classic' diffused light investigations: bench shaking/tapping/noise projections (Irene)
- 11:15 Scattered light investigations in LIGO (Robert)
- 12:00 Scattered light requirements for KAGRA and baffles design (Yoichi, Tomo) lunch
- 14:00 Diffused light in the time domain/glitches (Bas)
- 14:45 Some thoughts about Stray Light issues (Julien)
- 15:45 Higher order modes in filter cavities (Jan)
- 16:15 GEO tools: Omega, Non-Gaussian plots (Michal) (perhaps shift to Tuesday)
- 17:00 Scattered light investigations in GEO (past) (Harald et.al.)
- 17:45 DISCUSSION: goals of the week

Tuesday (at GEO):

- 9:30 Places to look in GEO (Jon)
- 11:00 DISCUSSION: experiments and simulations to do.
- 12:00 lunch
- 13:00 continue DISCUSSION
- 14:00 Start work: experiments, simulations

Wednesday (at GEO):

- 9:30 Feedback from yesterday: next experiments? what to analyze?
- 10:30 START work: experiments, simulations
- 13:00 lunch
- 14:00 DISCUSSION: Ideas not tried / new techniques
- 15:00 discuss / continue work
- 19:00-20:00: hike and dine

Thursday (at GEO):

- 9:30 Feedback from yesterday: next experiments? what to analyze? lunch
- 14:00 discuss / continue work
- flexible: hike and dine

Friday (at AEI, room 013, 3406 on LISA floor):

- 9:30 Feedback from yesterday: results? follow-up experiments? lessons learned?
- 12:00 workshop end
- lunch

B Participants

Figure 9 shows a picture of all of the participants.

Figure 9: Group photo. Back row: Kate Dooley, Robert Schofield, Hartmut Grote, Harald Lück. Middle row: Denis Martynov, Jon Leong, Emil Schreiber, Gabriele Vajente, Jake Slutsky, Jan Harms, Matteo Tacca, Romain Bonnand, Julien Marque, Mirko Priatelj. Front row: Tomo Akutsu, Bas Swinkels, Michal Was, Sheila Dwyer, Holger Wittel, Yoichi Aso, Irene Fiori.